SAND78-3266
Unlimited Release

MASTER

Preliminary Studies of Microchannel Plate Photomultiplier Tube Neutron Detectors for Flight Test Applications

K. W. Dolan

SF 2900 Q(7-73)

SAND78-8266
Unlimited Release
Printed October 1978

PRELIMINARY STUDIES OF MICROCHANNEL PLATE PHOTOMULTIPLIER TUBE NEUTRON DETECTORS FOR FLIGHT TEST APPLICATIONS

K. W. Dolan
Acceptance Technology Division 8444
Sandia Laboratories Livermore

ABSTRACT

Electrical, mechanical, thermal, and neutron response data indicate that microchannel plate photomultiplier tubes are viable candidates as miniature, ruggedized neutron detectors for flight test applications in future weapon systems.

ACKNOWLEDGEMENTS

It is a pleasure to acknowledge the essential technical assistance provided by R. J. Amaral, in performing the tests reported here. I am also indebted to R. O. Sundahl, for close cooperation in initiating and planning the tests, to W. E. Jorgenson for contributing holographic measurements of the mechanical response of the microchannel plates, to C. S. Hoyle for computational results on the mechanical properties of the plates, and to R. A. St. Hilaire for the design of mechanical fixturing.

CONTENTS

ILLUSTRATIONS

PRELIMINARY STUDIES OF MICROCHANNEL PLATE PHOTOMULTIPLIER TUBE NEUTRON DETECTORS FOR FLIGHT TEST APPLICATIONS

Introduction

Microchannel plate photomultiplier tubes are being evaluated for possible application to flight test pulsed neutron diagnostics. A miniature, ruggedized, moderately high gain (10^4-10^6) tube is required that can withstand extreme acceleration and vibration, and provide a signal during vibration without gain changes. Accelerations in excess of 10,000 g, and vibrations up to 0.15 g^2/Hz at 20 to 2000 Hz are of interest. Present flight test instrumentation uses either the SA1690 photomultiplier tube, which is a conventional dynode tube, or a large area silicon photodiode to measure light output from a neutron sensitive plastic scintillator. The SA1690 is limited to accelerations less than 250 g and vibrations 0.1 g^2/Hz, 20 to 2000 Hz. The silicon photodiode has withstood very high acceleration and vibration environments but gives relatively low signals, of the order of nanoamps, at the flux levels of interest.

Microchannel plate (MCP) technology is relatively new with only a few investigations reported on photomultiplier tube applications. Because of their small size, high current gain, and fast response characteristics, MCP's are particularly well suited for use in high gain imaging devices, and in very fast, moderately high gain, photomultiplier tubes (PMT's). The microchannel plate acts as the multiplying element in the PMT application in place of the conventional dynode chain. The electronic gain of MCP's may be 10^4 to 10^7 depending on the design and applied voltage. This compares to gains of 10^6 to 10^{10} with conventional high gain dynode tubes. Transit time spread in the MCP element is less than 100 ps, nearly an order of magnitude better than that of dynode tubes. Rise times as low as 250 ps have been obtained with specially designed MCP PMT's.[1]

The MCP element is a two dimensional parallel array of small channel electron multipliers (CEM's) consisting of hollow glass cylinders fused together (see Figure 1). The i.d. of each cylinder may be 10 to 40 μm, and the length, 0.5 to 2.0 mm. Each cylinder has a resistive secondary emissive coating on the inside surface so that an electron entering the input end of a CEM will receive multiplication of 10^4 to 10^7, depending on the applied voltage and length to diameter (L/D) ratio. Multiplication results from cascade action in which primary electrons collide with inner wall emissive surfaces and cause several secondary electrons to be emitted. Electrons are accelerated down the channel by an axial field and strike the channel walls due to the surface normal velocity component attained at emission. The cascade multiplication process continues until the end of the channel is reached or gain saturation occurs.

The MCP element does not suffer from gain changes during vibration as do conventional dynode tubes due to dynode displacements. The MCP is also unaffected by axial magnetic fields as high as 900 to 2000 gauss as compared to gain changes in conventional dynode tubes at 1 gauss. The transverse magnetic field that reduces the d. c. gain of MCP's to half its original value is as high as 500 to 800 gauss.[1] The small size of the MCP element, 0.5 to 2.0 mm thick and arbitrary diameter, lends itself to miniaturization of PMT's, which is a requirement for our applications.

Prior to receipt of custom designed MCP PMT's on order from ITT* that incorporate miniaturization and ruggedization features, a consignment lot of MCP night vision and image enhancement tubes was received for preliminary studies. The consignment tubes are similar to the ruggedized, higher gain tubes on order, and allowed preliminary evaluation of performance characteristics to be expected of the custom MCP tubes. Performance characteristics of interest in our preliminary assessment are optimum bias voltages, leakage currents, internal capacitance, noise levels, fast time response, neutron response, and saturation conditions. A number of MCP elements, 0.5 mm thick by 24 mm diameter (18 mm diameter active area), were also received for mechanical tests including yield pressure, Young's modulus, and Poisson's ratio. The results of electrical, mechanical, and environmental tests on the consignment parts are the subject of this report.

Test Results

A. Electrical Tests (Static)

1. Anode Capacitance

The anode capacitance was measured with an ECD C-meter.** The mean value of the measurements on four separate tubes was 14 ± 1 pf. The total MCP area, 4.5 cm^2, and MCP to anode separation distance, 0.1 cm, would imply a theoretical value of only 4.0 pf. It is assumed that geometry effects and the ring contact to ground capacitance (approximately 3 pf) account for the difference. The mean value for the capacitance of the MCP element from four separate measurements was 66 ± 6 pf, and the mean value of the photocathode to MCP capacitance was 37 ± 2 pf.

2. Dark Current

The dark current was measured at room temperature (22°C) using a Keithley Model 616 Digital Electrometer.† The voltage distribution applied, as recommended by ITT, was

---

* International Telephone and Telegraph, Electro-Optical Products Division, Fort Wayne, Indiana

** ECD Corporation, Cambridge, Mass.

† Keithley Instruments, Inc., Cleveland, Ohio

180 V photocathode to MCP, and 300 V MCP to anode. Battery supplies were used to avoid ground loops and anamolous leakage currents. Circuit ground was established by connecting the inner shield of the triaxial electrometer input to earth ground. The value obtained for anode dark current was approximately 0.1 nA.

3. Rise Time and Fall Time

Rise time and fall time measurements were made using a pulsed LED light source with peak spectral output at 550 nm. The pulse shape of the LED source was characterized with an EGG 585-66 photomultiplier tube* using a 50 ohm load and a Tektronic 7844 oscilloscope with 7A15A amplifier.** The EGG PMT is capable of delivering currents up to 1 mA as a linear function of input without distorting pulses, where rise times are greater than 10 ns. The bandwidth of the 7A15A amplifier is 80 MHz, allowing measurement of rise times as fast as 2.5 ns. The RC time constant of the EGG PMT system was estimated to be 9 ns based on the measured 60 pf anode capacitance of the PMT, 120 pf cable capacitance, and 50 ohm load.

Pulse shape measurements of the the LED source output with the EGG PMT system gave a 10-90% source rise time of 45 ns, a 10-90% fall time of 200 ns, and a pulse width (full width at half maximum) of 140 ns. The uncertainties in these values from error of measurement (e.g., from reading scope trace records) was ± 10 ns. The PMT measurements were taken at peak currents of 0.4 and 0.6 mA. Pulse shape distortion was observed at peak currents greater than 1.0 mA due to space charge limiting in the EGG PMT, as anticipated from the manufacturer's data sheet.

Response of an MCP tube to the LED pulsed light source was determined using the same scope/amplifier system and 50 ohm load. The entire sensitive area of the MCP photocathode was illuminated nearly uniformly so that no finite area element of the MCP would be driven to saturation. Pulse shapes remained undistorted over the range of peak currents obtained in these measurements, from 1.0 to 10.0 mA. The measured rise time was 35 ns, fall time was 200 ns, and pulse width 130 ns. The rise time and pulse width are slightly smaller than the PMT results, although the differences are within experimental errors. Pulse shapes remained undistorted for peak currents as high as 10.0 mA, the maximum signal obtained here. The maximum signal was dictated by power limitations of the LED, and uniform

* EG&G, Inc., Electro Optics Division, Salem, Mass.

** Tektronic, Inc., Beaverton, Oregon

illumination requirements restricting source to detector separation distances to greater than 10 cm. The integrated charge output from the 10.0 mA signal was 1.5 nC which corresponds to a charge density of 0.6 nC/cm^2 for the 18 mm diameter active area. This approaches the value of 0.8 nC/cm^2/pulse which is the anticipated level for onset of saturation effects.

4. Threshold Signals

Threshold signals were estimated in two ways. First, the threshold signal was defined from statistical arguments to be six times the root mean square (rms) noise signal. Since noise signals have a Gaussian distribution about zero voltage, and the rms value is the standard deviation (σ) of this distribution, this criterion places the threshold for signal measurements at the 6σ level. Using this criterion, the threshold signal was determined from noise level measurements to be 1.3 mV for a 50 ohm load, and 2.5 mV for a 500 ohm load.

In the second method, a subjective judgment was made from observations of many signal pulses that the threshold signal should be twenty times the rms noise value. This gives a statistical uncertainty from noise contributions of just 5% for the threshold signal defined in this manner, as compared to 17% for the 6σ criterion. Using the subjective criterion, threshold signals were determined to be 4.3 mV for a 50 ohm load, and 8.3 mV for a 500 ohm load.

5. Saturation

Saturation effects are the result of electron depletion of channel emission surfaces due to large input signals at high gain. Several milliseconds are required to restore distorted wall potentials to equilibrium following a saturation event because of the high resistivity of the MCP material. The visible effect of saturation is pulse distortion in the form of "pulse droop." A rectangular input pulse, for instance, will be output under saturation conditions as a pulse that decays with time, i.e., pulse droop.

To investigate this effect, the same LED light source was used, but power to the source was provided by an HP-214A Pulse Generator.* A pulse width of approximately 6.5 μs was chosen for these measurements to match the pulse width of a commercial neutron generator described in the next section for neutron response measurements. Both the rise time and fall time of the LED source with the pulsed generator supply were approximately 0.2 μs. Most of the saturation data was taken using a load resistor of 500 ohm, although a

* Hewlett-Packard, Palo Alto, Ca.

few data points were taken with a 50 ohm load for comparison. Special care was taken to eliminate extraneous background light, since constant current in the MCP tube caused by background light contributes to saturation effects.

Scope traces that show the response of an MCP tube to rectangular input light pulses of increasing intensity are given in Figure 2. At low intensities, the output pulse has an undistorted rectangular shape, as shown in Figures 2a and 2b. At higher intensities, the pulse shape is distorted, exhibiting pulse droop, as shown in Figures 2b and 2c. The amount of pulse droop, i.e., percentage deviation from a rectangular signal shape, is plotted in Figure 3 as a function of integrated output charge. We see that there is essentially no distortion below an integrated charge of 0.05 nC/cm^2, less than 4% distortion below 0.4 nC/cm^2, and less than 6% distortion below 1.0 nC/cm^2. Above 1.0 nC/cm^2 the percentage distortion increases dramatically, approaching an asympototic value near 3.5 nC/cm^2. This data shows that the onset of saturation occurs at approximately 1.0 to 1.5 nC/cm^2/pulse. The data is independent of the choice of load resistor, 50 ohm as compared to 500 ohm, as the data from both load resistors give good agreement in defining the saturation curve.

6. Neutron Signal

The MCP tubes were optically coupled to NE-108 plastic scintillators* for the neutron response measurements. Scintillation photons produced in the plastic as a result of neutron interactions cause photoelectron emission from the photocathode of the MCP tube. The photoelectrons are multiplied in the MCP element generating the signal pulse. The NE-108 scintillator has a broad spectral output that peaks near 570 nm, while the photocathode sensitivity has a broad maximum near 510 nm. The photocathode sensitivity at 570 nm for the MCP tubes used in the neutron response measurements (ITT Serial Nos. 3247D and 579-24), including the effect of face plate transmittance, was 33 mA/W. This converts to a quantum efficiency of 7.3%. Quantum efficiencies for the type of bi-alkali photocathode used in these tubes is normally closer to 10% at 500 nm, and peaks at a maximum efficiency of 20% near 410 nm. These higher quantum efficiencies should be realized in the custom tubes on order since a higher transmittance quartz faceplate will be used in place of the acceptance angle limited fiber optic faceplate.

The neutron source for the neutron response measurements was a G. E. Type 26A Controlatron Neutron Generator Tube.**

*Nuclear Enterprises, Inc., San Carlos, Ca
**General Electric Neutron Devices Dept., St. Petersburg, Fla.

The Controlatron is a highly stable, long life, pulsed source of 14 MeV neutrons with a peak output of approximately 3 x 10^{6} n/μs and a pulse width of 6 μs. The rise time of the source is approximately 1.2 μs and fall time 1.7 μs. The neutron flux was measured with a field test neutron detector, calibrated to 200 n/cm^2/μs/V at 15.2 cm (6.0 inches) from the source. The field test detector and the scintillation/MCP neutron detector were placed on opposite sides of the axisymmetric neutron source as shown in Figure 4. Lead shielding 3.2 mm (.125 in.) thick was positioned between the source and MCP detector to totally absorb x-rays produced by the source while transmitting more than 94% of the neutron flux. The distance from the center of the source to the volumetric center of the scintillator was varied to obtain different flux inputs. Scintillators of different sizes were also used to determine signal dependence on scintillator volume as a function of distance from the source. The scintillators used were right cylinders of dimensions 1.9 cm dia. x 2.9 cm (.75 in. x 1.125 in.) and 1.9 cm dia. x 5.1 cm (.75 in. x 2.0 in.). The direction of the incident neutron flux was along the cylindrical axis in all cases. An impedance matching charge sensitive preamplifier with unity gain was used to transmit the signal without distortion to an oscilloscope for photographic data recording. Load resistors of either 50 or 500 ohms were used in the output circuit.

Dual scope traces showing the response of a microchannel plate detector (MCPD), ITT Ser. No. 32470, and the field test detector, to neutron pulses with different pulse shapes are given in Figure 5. The MCP gain in this case was 280 at a bias of 850 V with a load resistor of 500 ohms. With the exception of statistical fluctuations in the signal traces of both detectors, the MCPD signal is seen to be an undistorted reproduction of the shape of the field test detector signal. Rise times and fall times are in agreement and are the characteristic times of the pulsed source. Signature characteristics of the signal traces seen with the field test detector are also observed with the MCPD. Both the 50 and 500 ohm output loads gave undistorted fast response traces of the output signal. A load resistor of 1000 ohms in the MCPD output circuit gave distorted pulse shapes, and was therefore eliminated from the remainder of the tests.

The responses of two MCPD's using different crystal sizes to neutron pulses of nearly constant intensity are given in Figure 6. Curves (a), (b), and (c) of Figure 6 were obtained with Tube No. 32470 at a gain of 280 using a load of 500 ohms for scintillators of sizes 5.4, 8.1, and 14.5 cm^3, respectively. The response is found to be directly proportional to the volume of the crystal with a volume sensitivity of 2700 n-cm/μs/mv.

Curve (d) of Figure 6 was obtained with Tube No. 579-24 at a gain of 5600 using a 500 ohm load and a 14.5 cm^3 scintillator. The volume sensitivity in this case is 750 n-cm/μs/mV. This differs from the result obtained with Tube No. 32470 by only a factor of 3.6, while the gain is a factor of 20 greater. The sensitivity should be inversely proportional to gain, all other factors being equal. The only other factor of importance should be the photocathode sensitivity which is nearly the same for the two tubes, 20.8 mA/W for Tube No. 32470, and 22.0 mA/W for Tube No. 579-24. The MCP active area is the same in both tubes, and both tubes use proximity focus for anode current collection. If the data from Tube No. 32470 is scaled to a gain of 10^4 we would obtain a volume sensitivity of 75 n-cm/μs/mV, while scaling the data from the 579-24 gives 420 n-cm/μs/mV. Thus a discrepancy of a factor 5.6 in the volume sensitivity data is noted here which remains unresolved. Special attention will be given this problem in testing the custom design tubes which are expected to have a gain of about 10^4. The strongest statement that can be made on volume sensitivity, based on the present measurements, is that it is approximately 100 to 400 n-cm/μs/mV at a gain of 10^4.

B. Thermal Tests

1. Preconditioning

A complete set of thermal tests was performed on Tube No. 32470 only. The tube was sealed in a light tight case and placed in a temperature chamber. The chamber was cooled by liquid nitrogen and heated by electrical elements. Electrical leads were brought through a port in the chamber door. The tube was preconditioned by thermal cycling to -40°C for 2 h and to +50°C for 2 h. Temperature changes were accomplished relatively slowly, with a period of approximately 1 h required to reach thermal equilibrium on each half cycle.

2. Dark Current

Dark current measurements were made as described in Section A2. Battery supplies were again used to eliminate ground loops. Dark current values were obtained as a function of temperature during thermal cycling between -40°C and +50°C. The results of these measurements are given in Figure 7. Between -40°C and ambient, 25°C, the dark current is observed to be nearly an exponential function of temperature. Above ambient, the dark current increases rapidly, departing from the simple exponential relationship.

3. Gain

The dependence of gain on temperature was determined by measuring the pulse height response of the MCP tube to a pulsed LED input signal. The LED was positioned outside the temperature chamber with the light output from the LED transmitted through a window in the chamber door to illuminate the MCP tube. Dry nitrogen was passed over the window to eliminate frost formation on the outside, and a dry nitrogen atmosphere inside the chamber eliminated frost formation on the inside chamber window and tube window. The pulse response of the MCP tube to the constant amplitude LED input signal at different temperatures is shown in Figure 8. The pulse shape remains unchanged while the pulse height decreases with increasing temperature. Since pulse height is a direct function of gain, the change in gain can be obtained directly from this data. The percentage gain change as a function of temperature, normalized to zero at 25°C, is given in Figure 9. The slope of the gain change from -35°C to -5°C is approximately -0.3% per °C. From -5°C to +25°C, the gain is nearly independent of temperature, and above +25°C the slope of the gain change is approximately -1.0% per °C. Decreased gain with increasing temperature is an effect of the negative temperature gradient of resistivity. The lead-oxide emitting surfaces of the microchannel plate become poorer emitters with decreasing resistivity (increasing conductivity).

C. Mechanical Tests

1. Static Pressure

MCP elements, 24 mm (0.96 in.) diameter by 0.55 mm (0.022 in.) thick, were epoxy bonded to special support fixtures as shown in Figures 10a and 10b for the static pressure tests. A pressure differential was applied by evacuating one side of the MCP element with the other side at atmospheric pressure. The MCP surface at atmospheric pressure was covered with a thin plastic foil, 0.0025 mm (0.001 in.) thick, to provide a vacuum seal. A reflective coating was also applied to the plastic foil to allow optical measurements of surface deflections. The pressure differential could be varied between 0 and 14.7 psi by adjustment of a needle valve to atmosphere in the vacuum line.

Two MCP elements mounted on pseudo-fixed boundary supports (see Figure 10b) were taken to failure at pressure differentials of 13.0 and 13.5 psi, respectively. A third MCP element on a fixed boundary support (Figure 10a) withstood the maximum pressure differential of 14.7 psi without failing.[3] Equating pressure differential to force of acceleration, using an areal density of 70 mg/cm^2 for the MCP element, the 13.0 and 13.7 psi failure levels correspond to accelerations of 12,900 and 13,400 g, respectively, while the 14.7 psi differential corresponds to 14,500 g. Holographic measurements of surface deformation caused by the applied pressure differential are being analyzed

and additional data are being taken to establish elastic constants of the MCP element. Preliminary results from the fixed boundary data[3] indicate a Young's Modulus of 1.2×10^6 psi, assuming a Poisson's ratio of 0.2 to 0.3.

2. Vibration

Sinusoidal vibration tests of the MCP element to determine vibration modes and resonance frequencies were planned but not completed for this report. However, theoretical calculations[4] using the Young's modulus and Poisson's ratio given in the previous section, indicate the first resonance frequency of the zeroth order harmonic to be 5800 Hz. This assumes fixed boundary conditions for a 2.49 cm (0.98 in.) diameter by 0.051 cm (0.020 in.) thick plate. The ring contact surface outside 2.18 cm (0.86 in.) is held fixed for the calculation, while motion of the plate inside 2.18 cm is undamped. The MCP element is assumed to be composed of porous glass with a mean density of 1.38 g/cm^3 (42.3% dense) to a diameter of 1.98 cm (0.78 in.), joined to an outside ring of Corning 8161 glass with a density of 3.29 g/cm^3 and an o.d. of 2.49 cm. The Young's modulus is assumed to be 1.2×10^6 psi for the porous glass, and 7.8×10^6 psi for the solid glass. The first resonance at 5800 Hz has a simple dished displacement shape with no nodes. The second resonance frequency of the zeroth harmonic with one node is at 22,000 Hz, while first resonance frequencies of higher order harmonics are even higher.

3. Acceleration

An MCP element was accelerated on a centrifuge to determine the dynamic g-loading failure level. The MCP was epoxy bonded to a special support as shown in Figure 10c for the centrifuge tests. The MCP element was positioned 7.6 cm (3.0 in.) from the central axis of the centrifuge. An LED mounted on axis provided a diagnostic signal for monitoring the mechanical integrity of the MCP element. The constant light output from the LED was measured with a phototransistor positioned on the same radial arm as the MCP, and shadowed by the partially transparent body of the MCP. A collimation aperture, which also acted as a debris shield, was placed between the phototransistor and MCP to accept only the direct light signal transmitted through the MCP. Electrical output from the phototransistor was brought through slip ring contacts and measured with an ammeter. A change in the phototransistor current was assumed to indicate structural failure of the MCP element.

The acceleration tests on the MCP element were started at 1000 rpm (85 g) and continued in increments of 1000 rpm until

3000 rpm (770 g) was reached.* The tests then proceeded in increments of 500 rpm up to 5000 rpm (2130 g). Above 5000 rpm, increments of 100 rpm were used. Failure of the MCP element occurred at 10,750 ± 100 rpm, or 9850 ± 200 g. A reduction in the phototransistor current was observed at this point, and the test unit was immediately decelerated to rest. Visual inspection showed that the MCP element had broken into many small pieces that had partially blocked the collimator aperture causing loss of signal. The failure level observed in this test is comparable to the failure level of 13,000 g inferred from the static pressure tests.

D. Electrical Tests (Dynamic)

1. Random Vibration

An MCP tube was subjected to random vibration at 0.15 g^2/Hz from 20 to 2000 Hz to determine vibration effects on noise and signal response. The tube was potted in wax to provide good mechanical coupling without amplification. The potted assembly was mounted on a vibration fixture, and the fixture was attached to a vibration table for testing. The table provided motion in the vertical direction only, so that vibration along different axes of the tube was obtained by reorienting the tube in the fixture.

Effects of vibration on noise, pulse shape, and gain were determined by monitoring the response of an MCP tube under vibration to a pulsed LED light source. The LED source was mounted on a stationary framework adjacent to the vibration table. For vibration along the tube axis, i.e., normal to the tube window, the LED was mounted above the table and focused so that the beam intersecting the MCP tube was smaller than the sensitive area of the MCP element. This arrangement provided an MCP signal that was independent of relative displacement toward or away from the light source. For vibration normal to the tube axis, the LED source was mounted to the side of the table, in line with the axis of the tube. For this case, the light beam was diffused so that it was larger than the MCP active area giving uniform illumination of the MCP at all displacements. This arrangement again provided an MCP signal that was independent of displacement. Care was taken in both arrangements to avoid light levels that would cause saturation effects in the MCP tube.

*Centrifugal acceleration is proportional to the radius to the first power and to the rate of revolution to the second power with a constant of proportionality of 2.84×10^{-5} g/in/rpm^2.

Scope traces of the MCP response obtained under vibration-free conditions were used as standards for comparison to traces of the MCP under vibration. The results gave no evidence of pulse shape or amplitude changes over the entire range of vibration frequencies impressed on either axis. Similarly, no changes were observed in noise levels under vibration conditions as compared to vibration-free conditions.

2. Acceleration

An MCP tube was mounted on the radial arm of the centrifuge at 7.6 cm (3.0 inches) from the central axis with full electrical connections to determine the effect of acceleration on signal response. An LED pulsed light source mounted on the central axis of the centrifuge provided an input signal for the MCP tube. Electrical connections to the LED and MCP tube were made through slip ring contacts. Since the MCP tube was not ruggedized, loss of signal was expected at some point in the acceleration test before the failure level of the MCP element was reached. In particular, the weakest link in the system was expected to be the internal electrical contact to the MCP element which is a wavy washer spring contact. The spring contact was expected to compress under acceleration resulting in loss of electrical contact with the MCP element. Loss of signal did, in fact, occur between 4000 and 4200 rpm, or approximately 1400 g.

Deceleration below this level restored the signal, while repetitions to 1400 g caused successive loss of signal, indicating loss of electrical continuity through the spring contact. A fixed contact support to be used in the ruggedized design should raise the loss of signal level to the MCP failure level. A significant amount of noise was observed in the output signal due to noise generated in the slip ring contacts. However, the pulsed shape did not appear to be distorted.

Summary and Conclusions

Preliminary evaluations were made on the performance characteristics of microchannel plate photomultiplier tubes which are under consideration as detectors for pulsed neutron flight test diagnostics. Electrical, mechanical, and thermal response measurements were made on a consignment lot of MCP night vision and image enhancement tubes prior to receipt of custom designed, ruggedized MCP photomultiplier tubes. The consignment tubes have the same basic electrical design as the custom tubes, and provide an adequate basis for preliminary evaluations of MCP tube characteristics.

MCP tubes have a very fast time response with rise times of the order of 200 to 500 ps, and fall times less than a few ns, depending on the

load resistor. Measured threshold levels, using a criterion of twenty times rms noise for 5% statistical uncertainty at threshold, were approximately 4 mV for a 50 ohm load, and 8 mV for 500 ohms. Onset of saturation causing pulse distortion occurred at integrated charge outputs greater than 1.0 nC/pulse. Neutron response of MCP tubes optically coupled to plastic scintillators were found to be directly proportional to the volume of the scintillator. Measured neutron sensitivities, normalized to unit scintillator volume and to a tube gain of 10^4, were 100 to 400 n-cm/μs/mV, using a load resistor of 500 ohms. Thus, a 5.3 cm^3 scintillator (3/4 inch diameter by 3/4 inch thick), for instance, has a sensitivity of 20 to 80 $n/cm^2/\mu s/mV$ at an MCP gain of 10^4 into 500 ohms. Improvements in the photocathode efficiency and window transmittance of the custom tubes should improve the sensitivity by about a factor of 20. Threshold levels with the anticipated improved sensitivity using a 5.3 cm^3 scintillator, a tube gain of 10^4, and 500 ohm load, would be of the order of 10 to 30 $n/cm^2/\mu s$. Onset of saturation for an MCP-PMT with 1.8 cm diameter MCP element, and the 6 μs wide pulse used here, would be approximately 300 to 800 $n/cm^2/\mu s$, giving a dynamic range of about 30 from the threshold.

Mechanical test results showed that (1) the MCP element survived static pressure differentials corresponding to a g-loading of approximately 13,000 g, (2) dynamic g-loading failure in a centrifuge test occurred at 9600 g, and (3) vibration loading at 0.15 g^2/Hz in the frequency range 20-2000 Hz produced no observable gain changes. Temperature tests showed that the tube gain has a negative temperature gradient, exhibiting a -7% gain change from -45°C to +25°C, and a -23% gain change from +25°C to +50°C.

With the exception of the latter temperature effect, which may be correctable by using temperature compensating electronics, the present results give a preliminary indication that MCP tubes are viable candidates for flight test pulsed neutron detectors. Rise times and fall times of MCP tubes are less than 1 ns. The dynamic range is approximately 30 for a 6 μs wide pulse, while the threshold level is about 10 to 30 $n/cm^2/\mu s$ at a tube gain of 10^4, using a 500 ohm load and a 5.4 cm^3 plastic scintillator. Failure levels of the MCP element under acceleration are of the order of 10,000 g. Random vibration produces no observable gain changes or signal distortions at 0.15 g^2/Hz in the frequency range 20 to 2000 Hz, while the first resonance frequency is predicted to be 5800 Hz.

REFERENCES

1. B. Leskovar, "Microchannel Plates," Physics Today, pp. 42-48, November 1977.

2. D. H. Ceckowski, ITT Electro-Optical Products Division, Fort Wayne, Indiana, private communication.

3. W. E. Jorgenson, Sandia Laboratories Livermore, private communication.

4. C. S. Hoyle, Sandia Laboratories Livermore, private communication.

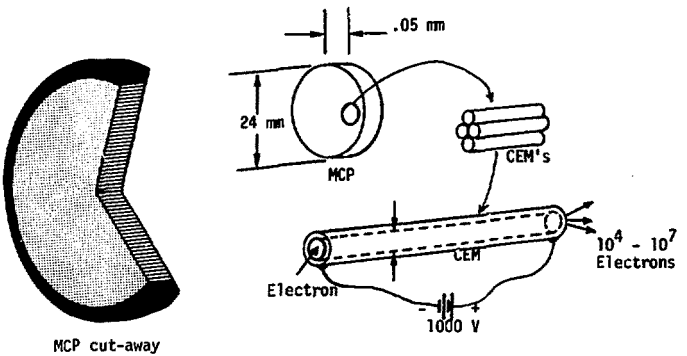

Figure 1.a. Schematic representations of microchannel plate (MCP) including cut-away and sectional views.

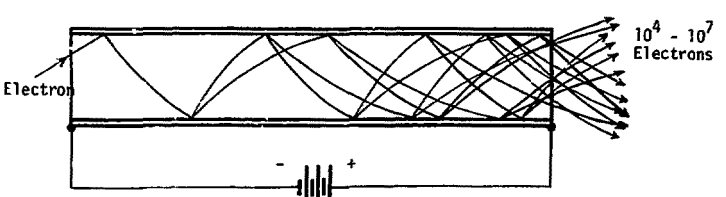

Figure 1.b. Schematic representation of channel electron multiplier (CEM) and electron multiplication process showing secondary emission from channel walls.

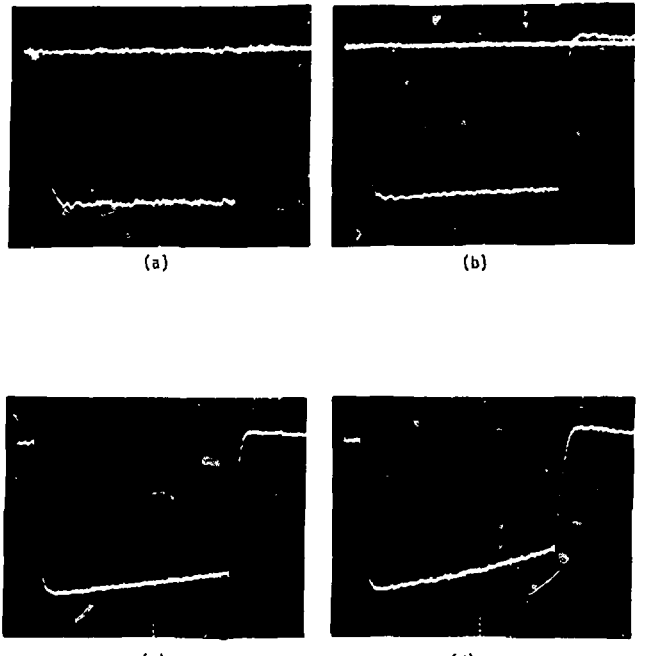

Figure 2. Scope traces showing "pulse droop" characteristic of MCP tube response to rectangular input light pulses of increasing intensity. Light pulses are 6.5 μs wide with a spectral distribution centered at 550 μm. Integrated charge output densities are (a) 0.025 nC/cm^2, (b) 0.17 nC/cm^2, (c) 1.45 nC/cm^2, and (d) 2.24 nC/cm^2, corresponding to 0%, 4%, 12%, and 26% pulse droop, respectively.

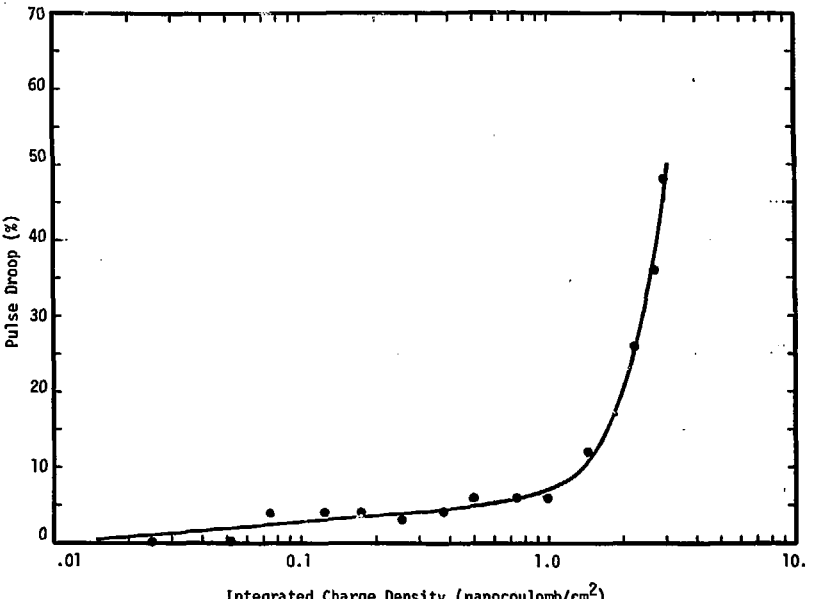

Figure 3. Pulse droop, i.e., percent deviation from rectangular shape, as a function of integrated output charge. Saturation effects in the MCP element cause large pulse distortion above 1.0 nC/cm^2/pulse.

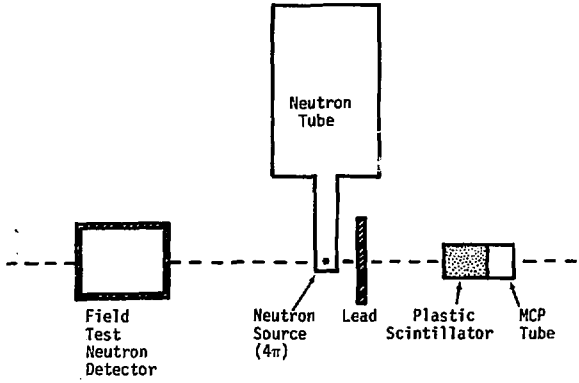

Figure 4. Schematic arrangement for neutron response measurements. Lead shielding between source and detectors asborbs X-rays while passing greater than 94% of incident 14 MeV neutrons. The field test detector is used for source normalization measurement of output rate and pulse shape, and is self-shielded with lead.

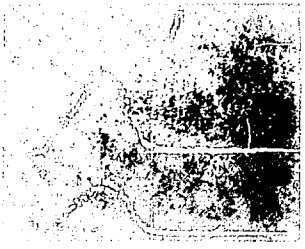

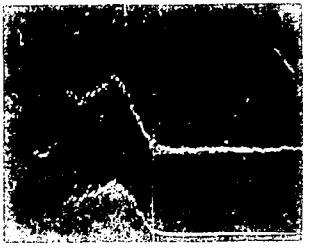

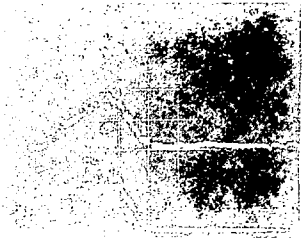

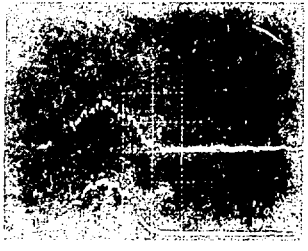

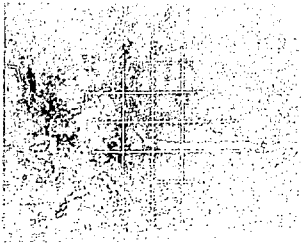

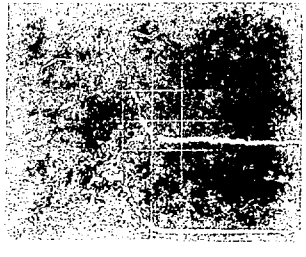

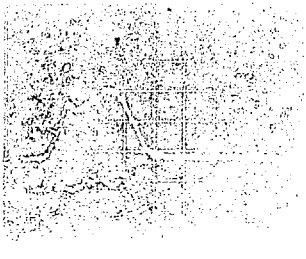

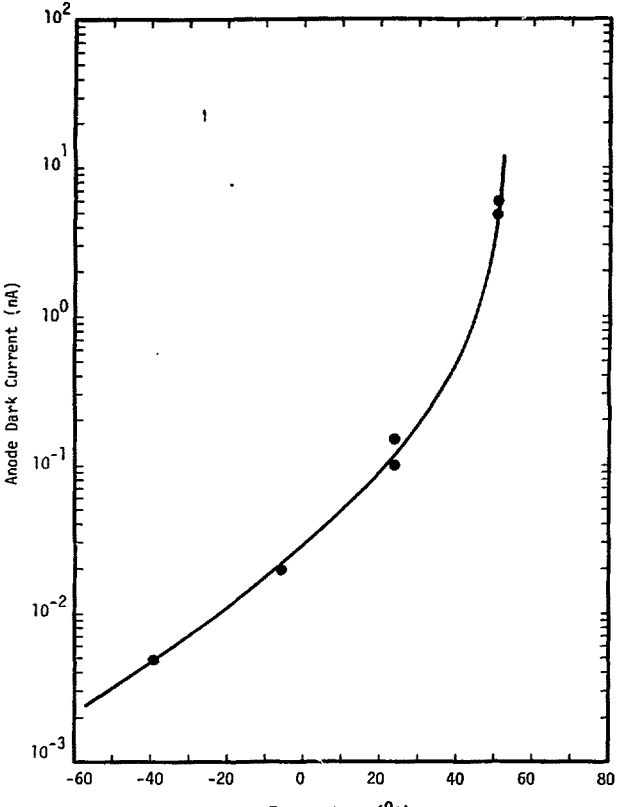

Figure 7. Anode dark current as a function of temperature. From -40°C to ambient, 25°C, dark current is nearly an exponential function of temperature (linear on the log-linear scale used here). Above ambient, the dark current increases faster than an exponential.

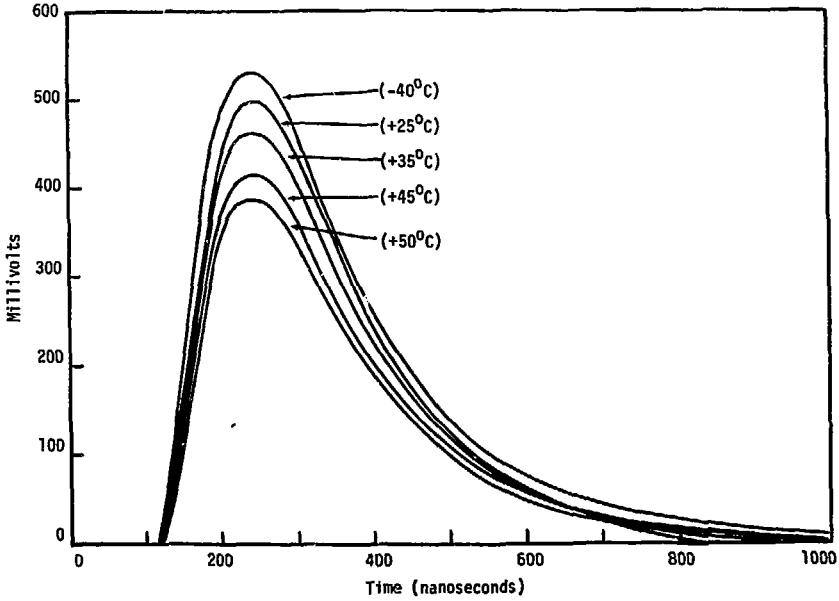

Figure 8. Pulse shape response of an MCP tube to a pulsed LED source of constant amplitude as a function of temperature. MCP amplitude decreases with increased temperature.

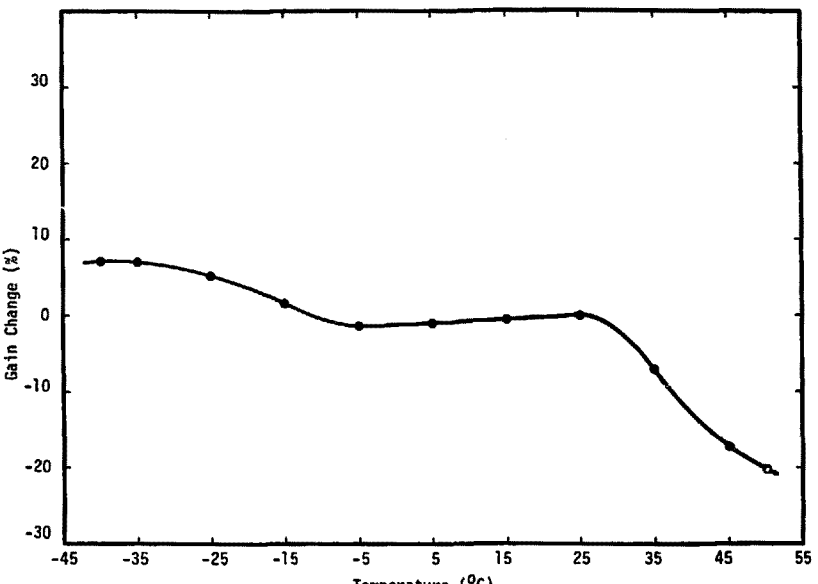

Figure 9. Gain changes as a function of temperature. The negative slope of the gain change curve, i.e., decreasing gain, is caused by the effect of decreased resistivity of the MCP element with increased temperature.

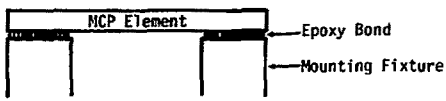

(a) Fixed Boundary Support Used in Static Pressure Test

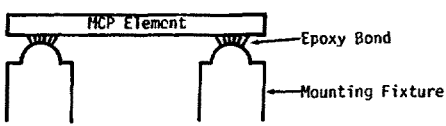

(b) Pseudo-Fixed Boundary Support Used in Static Pressure Test

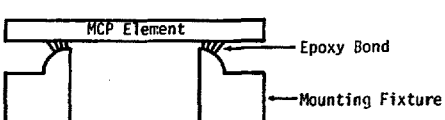

(c) Pseudo-Fixed Boundary Support Used in Acceleration Tests

Figure 10. Microchannel plate (MCP) mounting schemes for static pressure tests, (a) and (b), and acceleration test, (c).